

The partitioning of emulsifiers in o/w emulsions: A comparative study of SANS, ultrafiltration and dialysis

Kathleen Oehlke¹, Vasyl Haramus², Anja Heins¹, Heiko Stöckmann¹, Karin Schwarz¹

¹Institute of Human Nutrition and Food Science, University of Kiel, Kiel, Germany

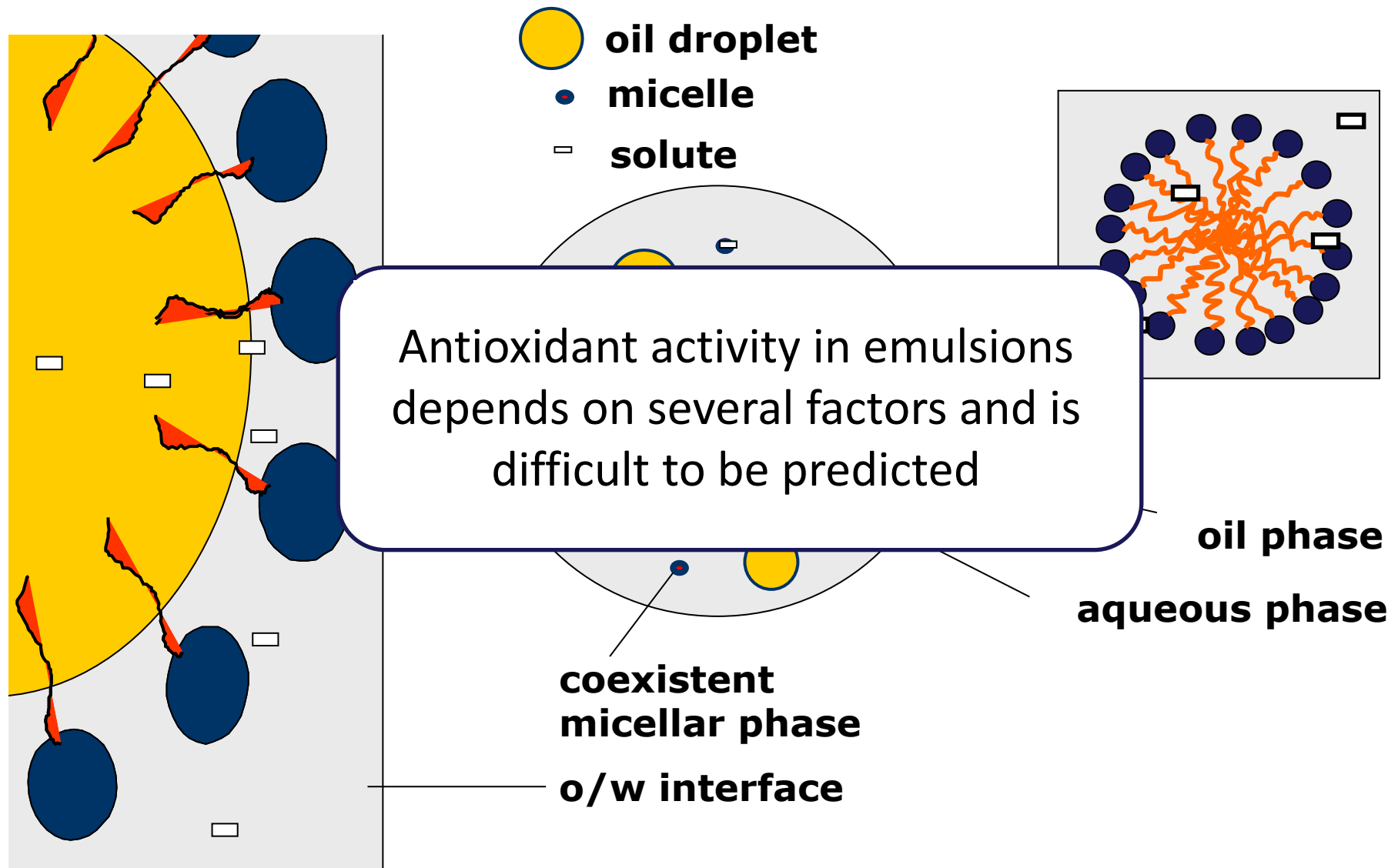
²Helmholtz-Zentrum Geesthacht: Zentrum für Material- und Küstenforschung, Geesthacht, Germany

31.01.2012 / Delft

Introduction – why SANS

- Food is usually a complex matrix with different phases / constituents and hence different structures
- Phases or structures represent reaction sites for chemical reactions that are relevant e. g. for storage stability
- To understand reactions in food matrices it is important to know the structures

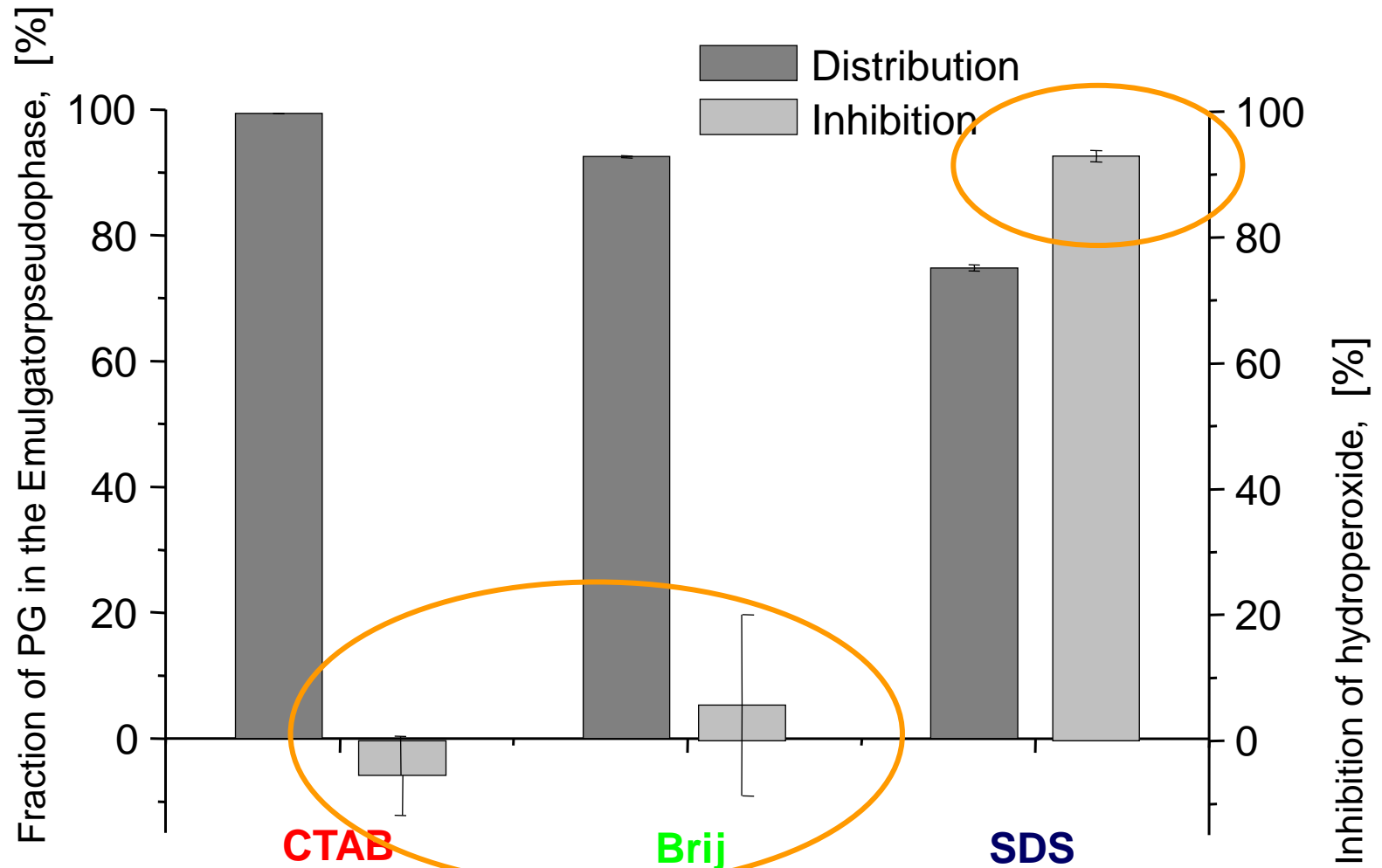
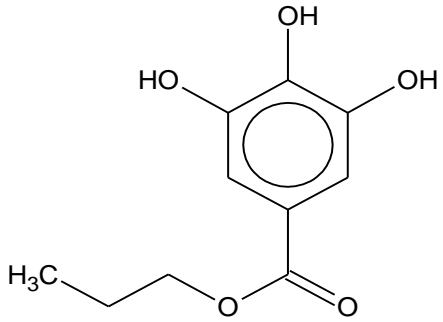
Solubilisation and reactions sites in o/w emulsions



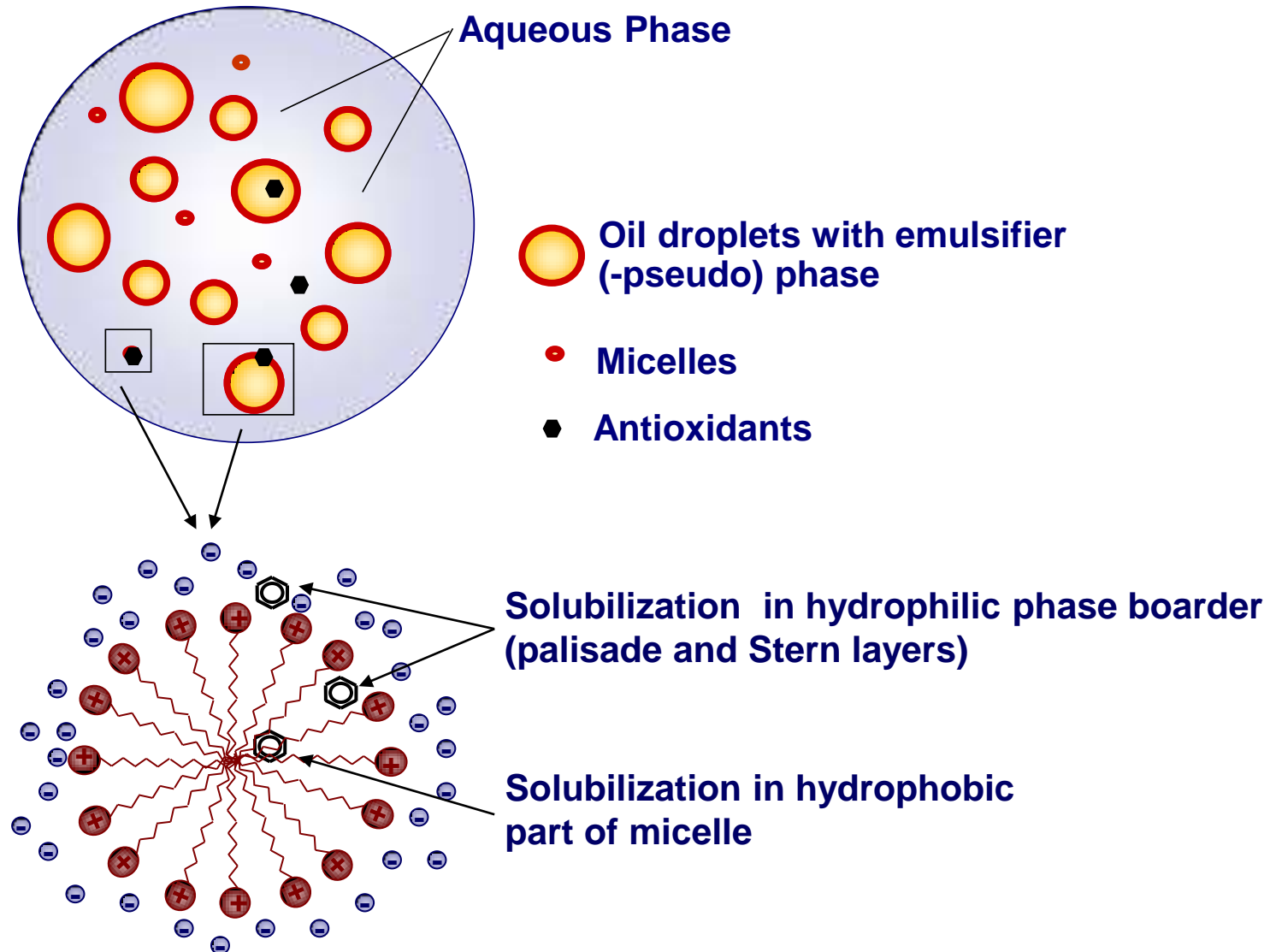
Lipid oxidation and antioxidant activity in emulsions

- Progress of lipid oxidation in emulsions depends on the type and concentration of the emulsifier
- Activity of antioxidants in emulsions depends on type and concentration of the emulsifier
- Not always correlated to the partitioning of the antioxidants

Activity vs. distribution of propyl gallate (PG) in different o / w emulsions



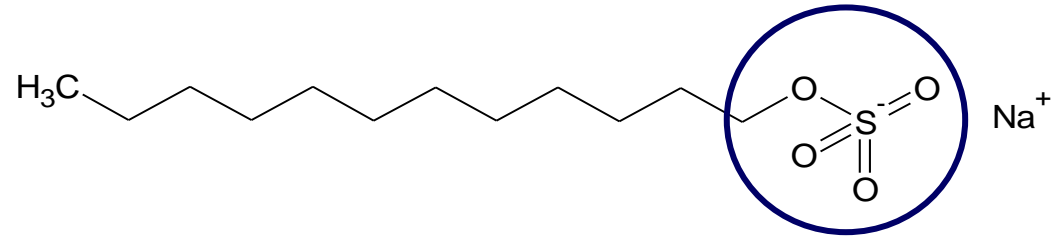
Localization of Antioxidants in Dispersions



Different Electrical Charge of Emulsifiers

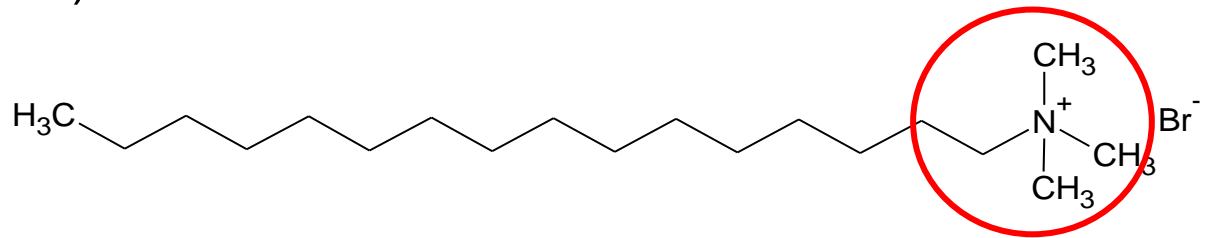
SDS

(Sodium dodecyl sulfate)
anionic head group



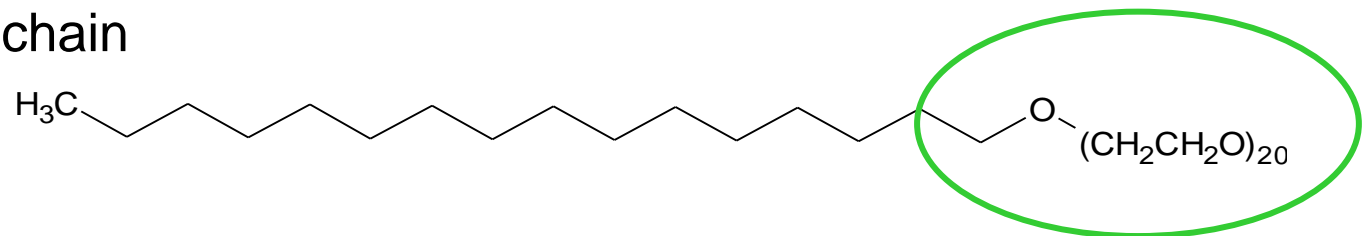
CTAB

(Cetyl trimethyl ammonium bromide)
cationic head group



Brij 58

(Polyoxyethylene-20-cetyl ether)
nonionic Polyoxyethylene-chain



Antioxidants: Gallate Esters

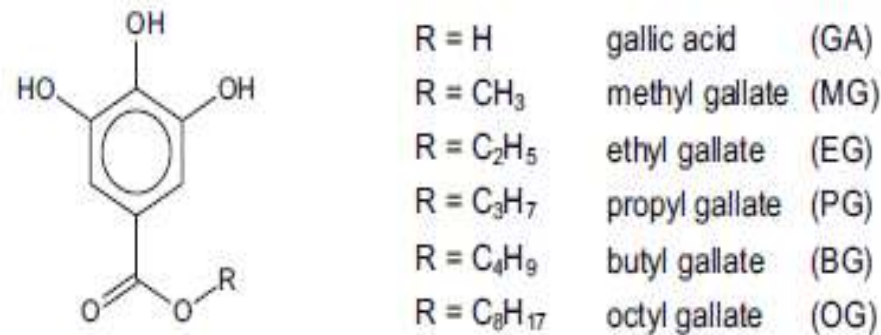
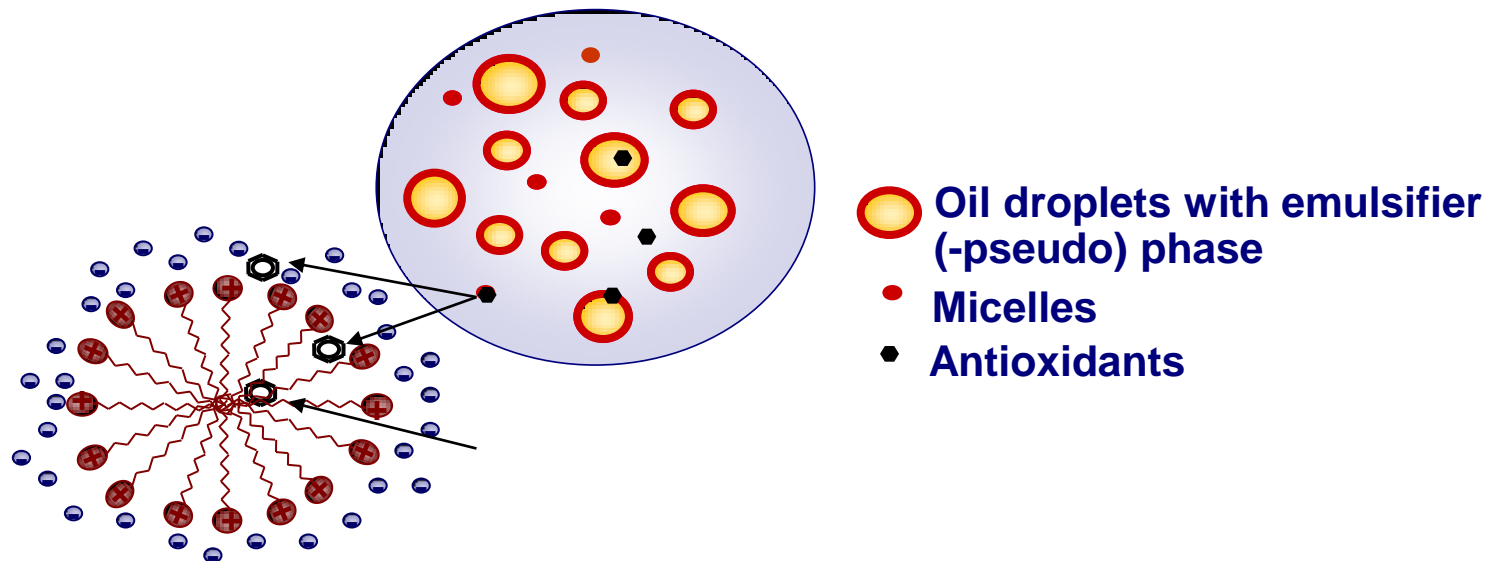


Fig. 1. Structures of gallates.

Sigma Aldrich, Seelze, Germany

Interaction between emulsifier and antioxidant at micellar solution i.e., effect of antioxidant on micelle formation and micelle structure.



Methods

Viscosity
 H₂O or D₂O
 25°C. Con

Critical m
 method Kr
 $\sigma = 69.7 \pm 0$
 $T = 20 \text{ }^\circ\text{C}$. **C**

SANS: SA
 $T = 25.0 \pm$
 Transform
function of $\rho_{CS,g}$, radius of gyration R_g , $\chi_{CS,g}$, mass of aggregate M (M_L).

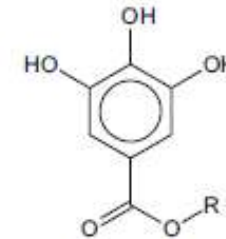
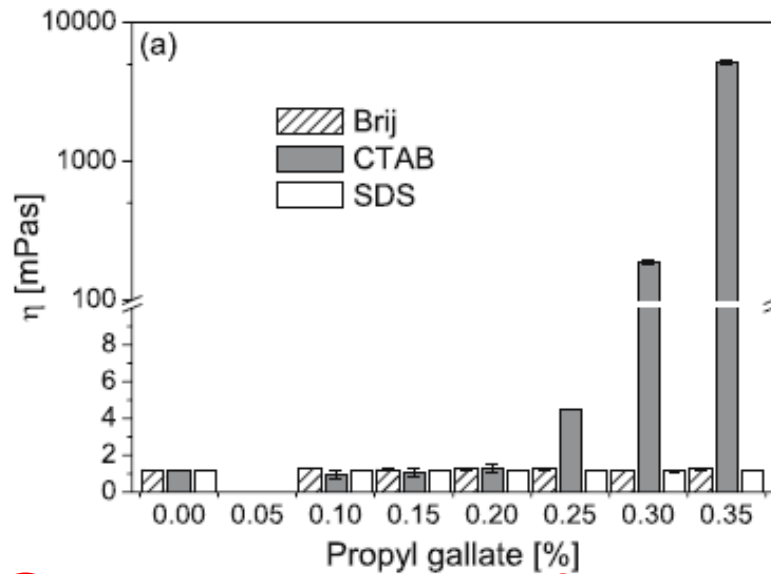


CVO 120.
 measured at
osity η .

num plate
 M , 5.0 pH,
 ntration. T

$Q = 0.25 \text{ } \text{\AA}^{-1}$.
 ct Fourier
istribution
function of $\rho_{CS,g}$, radius of gyration R_g , $\chi_{CS,g}$, mass of aggregate M (M_L).

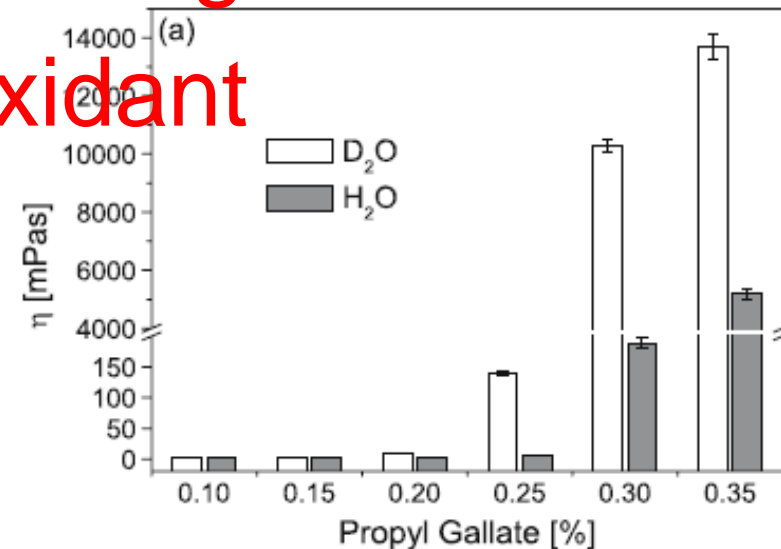
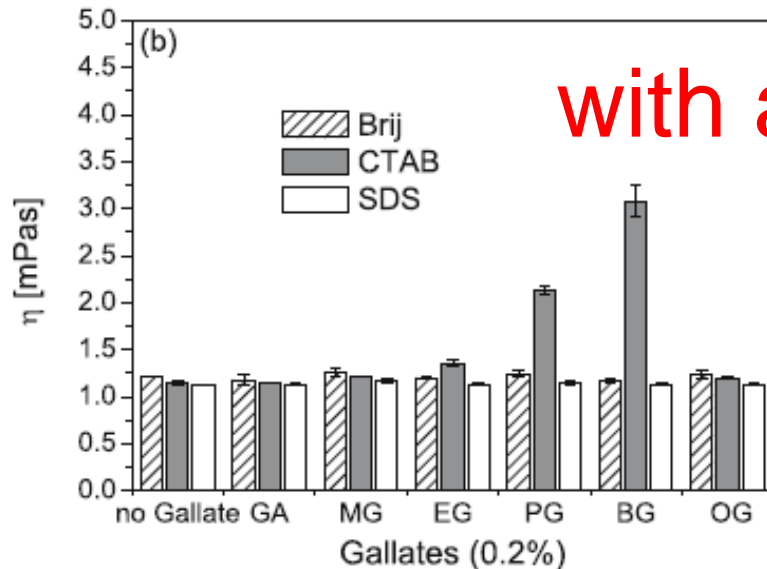
Viscosity: Concentration and Type of Gallates



- R = H gallic acid (GA)
- R = CH₃ methyl gallate (MG)
- R = C₂H₅ ethyl gallate (EG)
- R = C₃H₇ propyl gallate (PG)**
- R = C₄H₉ butyl gallate (BG)
- R = C₈H₁₇ octyl gallate (OG)

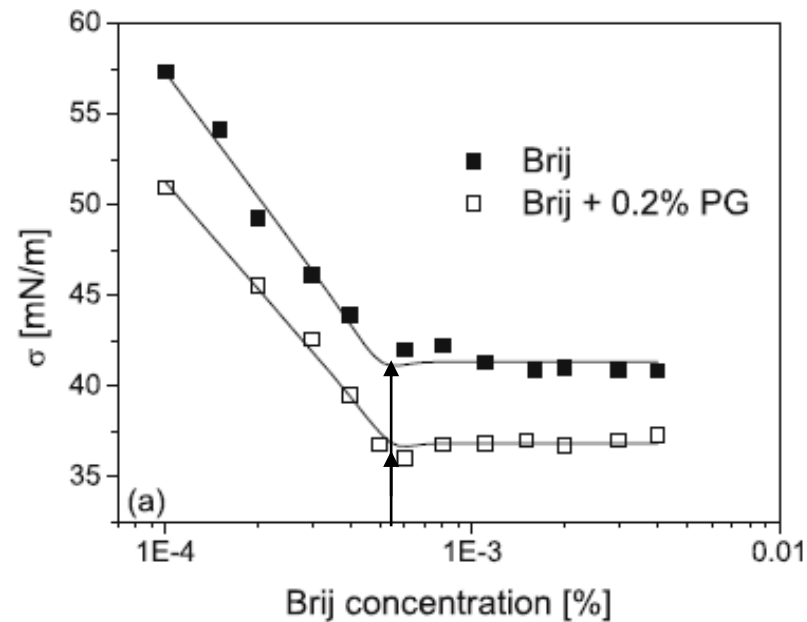
Fig. 1. Structures of gallates.

CTAB emulsifier shows strongest interaction with antioxidant



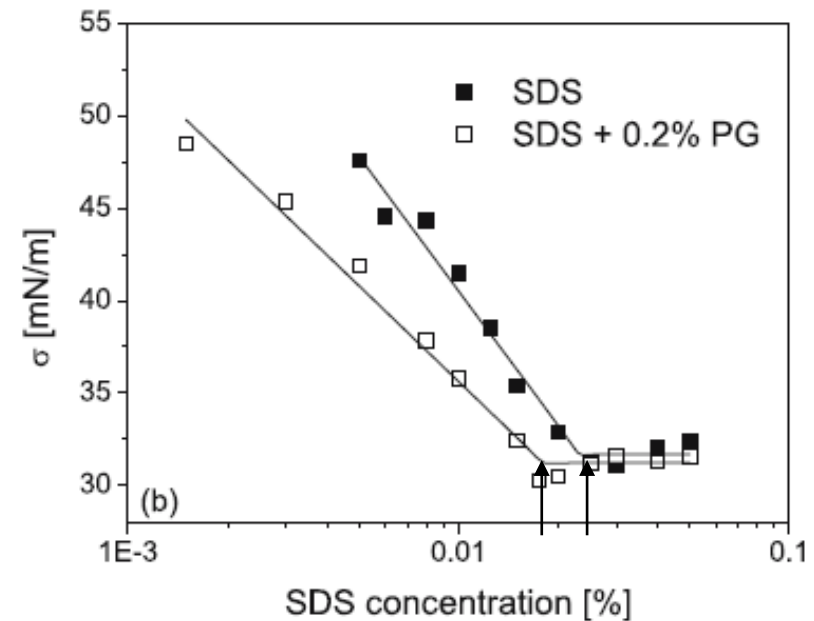
CMC and surface tension

Brij 58



Surface tension at CMC
is lower
CMC is constant

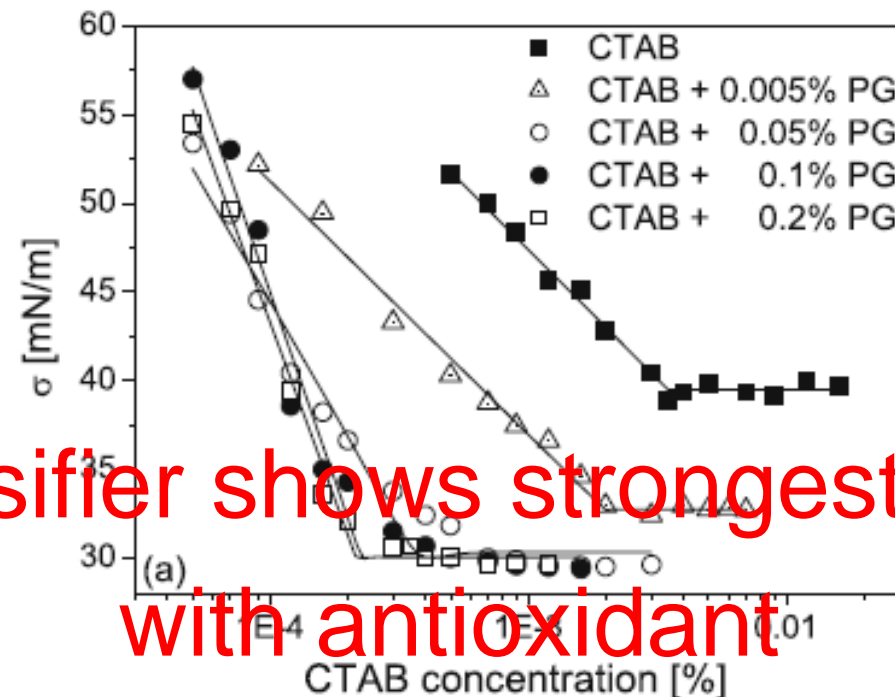
SDS



Surface tension at CMC
is constant
CMC is lower

CMC and surface tension

CTAB



CTAB emulsifier shows strongest interaction with antioxidant

Surface tension at CMC is lower

CMC is lower

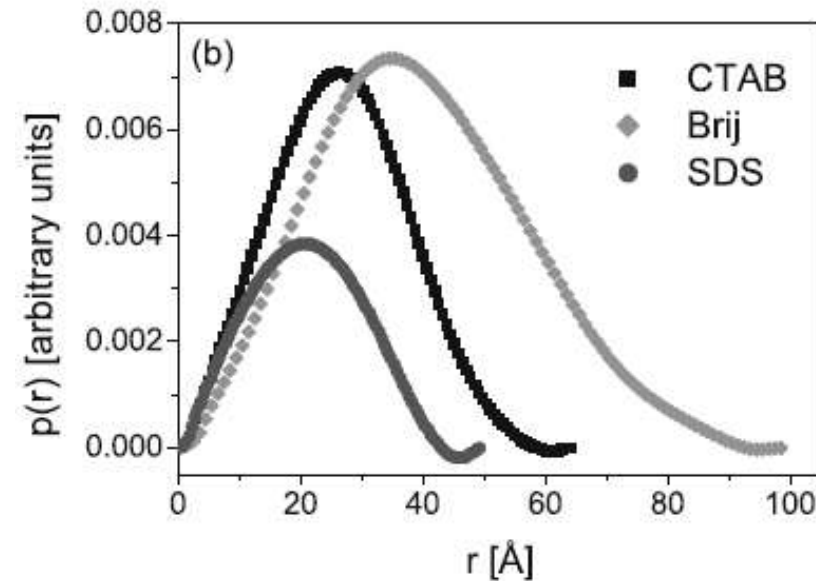
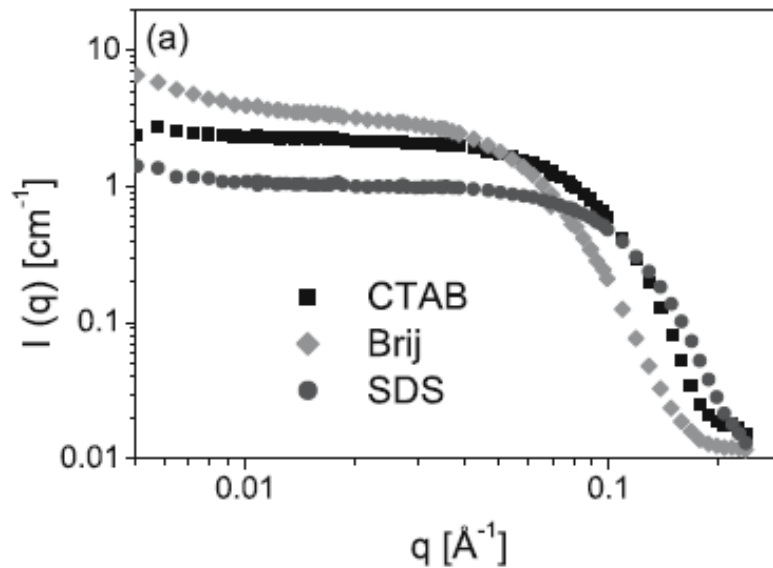
Concentration and type of oxidant play role

Antioxidants: CMC and surface area per molecule

Table 2 Determination of the cmc, specific excess surface concentration, and free energy of micellization of CTAB, Brij 58, and SDS in the absence and presence of selected antioxidants

	cmc[mg/L] ^c mean ± s.d. ^a	σ_{cmc} [mN/m] ^{cd} mean ± s.d. ^a	$\frac{\partial \sigma}{\partial \ln c_s}$ [mN/m] ^{ce} mean ± s.d. ^a	$\Gamma^* \cdot 100[\text{Å}^{-2}]^f$ mean ± s.d. ^b	ΔG_M° [kJ/mol] ^g mean ± s.d. ^b
CTAB	34.8 ± 2.00 ^α	39.5 ± 0.17	6.3 ± 0.24	0.8 ± 0.03	-21.0 ± 0.13
+ 0.005%PG	19.8 ± 1.70 ^β	32.8 ± 0.29	6.2 ± 0.25	0.8 ± 0.03	-22.3 ± 0.19
+ 0.05%PG	3.7 ± 0.40 ^η	30.3 ± 0.50	10.8 ± 0.84	1.4 ± 0.11	-26.1 ± 0.25
+ 0.1%PG	2.3 ± 0.20 ^ω	30.1 ± 0.59	18.3 ± 1.33	2.4 ± 0.18	-27.2 ± 0.20
+ 0.2%PG	2.2 ± 0.10 ^ω	30.1 ± 0.38	17.3 ± 0.83	2.3 ± 0.11	-27.3 ± 0.10
+ 0.005%GA	23.0 ± 1.90 ^{β,γ}	38.2 ± 0.28	6.0 ± 0.35	0.8 ± 0.09	-22.0 ± 0.19
+ 0.005%CA	21.1 ± 2.30 ^γ	36.8 ± 0.33	5.1 ± 0.34	0.7 ± 0.09	-22.1 ± 0.25
+ 0.005%SA	26.5 ± 2.70 ^β	39.1 ± 0.36	6.2 ± 0.41	0.8 ± 0.11	-21.6 ± 0.23
Brij	5.0 ± 0.30 ^α	41.4 ± 0.27	9.9 ± 0.61	2.6 ± 0.08	-28.0 ± 0.42
+ 0.2%PG	5.5 ± 0.20 ^α	36.9 ± 0.16	8.5 ± 0.33	2.2 ± 0.04	-27.8 ± 0.25
SDS	232.1 ± 19.1 ^α	31.7 ± 0.46	10.5 ± 0.76	1.4 ± 0.10	-16.2 ± 0.15
+ 0.2% PG	180.3 ± 14.4 ^β	31.2 ± 0.36	7.5 ± 0.37	1.0 ± 0.05	-16.7 ± 0.14

Antioxidants: Micellar size and shape



- Micelles are spherical in binary solution (emulsifier/acetic buffer)
- Addition of antioxidant gives sphere-rod transition for CTAB solution
- Addition of antioxidant gives minor changes for SDS and Brij

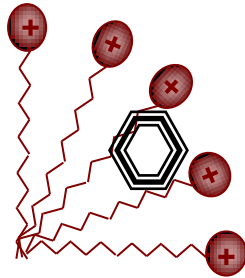
Micellar size and shape

Table 3 Calculations of the shape, size and aggregation number per micelle using to the fitted SANS data

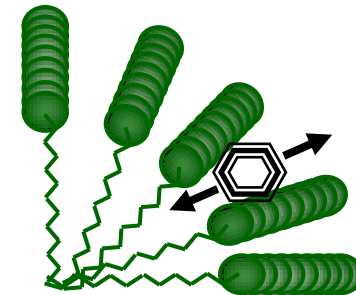
	shape	$R[\text{Å}]^d$ mean \pm s.d. ^a	$L_{\text{app}}[\text{Å}]^e$ mean \pm s.d. ^b	$R_{\text{cs}}[\text{Å}]^f$ mean \pm s.d. ^b	N_{agg}^g mean \pm s.d. ^c
1% SDS	sphere	$16.1 \pm 0.1^\alpha$			$80 \pm 1^\alpha$
+ 0.1% PG	sphere	$15.1 \pm 0.1^\beta$			$72 \pm 1^\beta$
+ 0.2% PG	sphere	$15.2 \pm 0.1^\beta$			$69 \pm 1^\gamma$
+ 0.3% PG	sphere	$15.0 \pm 0.1^\beta$			$68 \pm 1^\gamma$
1% Brij	sphere	$30.9 \pm 0.3^\alpha$			$73 \pm 1^\alpha$
+ 0.1% PG	sphere	$30.5 \pm 0.3^\alpha$			$74 \pm 1^\alpha$
+ 0.2% PG	sphere	$29.7 \pm 0.3^\beta$			$75 \pm 1^\alpha$
+ 0.3% PG	sphere	$29.2 \pm 0.3^\beta$			$75 \pm 1^\alpha$
1% CTAB	sphere	$10.5 \pm 0.1^\alpha$			$70 \pm 0^\alpha$
+ 0.1% PG	sphere	$23.8 \pm 0.1^\delta$			$155 \pm 0^\eta$
+ 0.15% PG	rod-like		$421 \pm 12^\lambda$	21.4 ± 0.1	944 ± 17^o
+ 0.2% PG	rod-like		$609 \pm 25^\rho$	21.6 ± 0.1	$1,414 \pm 10^\theta$
+ 0.25% PG	rod-like		$659 \pm 23^\sigma$	22.1 ± 0.1	$1,610 \pm 8^\tau$
+ 0.3% PG	rod-like		$712 \pm 19^\pi$	22.1 ± 0.1	$1,540 \pm 6^\sigma$
+ 0.35% PG	rod-like		$635 \pm 21^{v,o}$	21.8 ± 0.1	$1,525 \pm 8^\rho$
+ 0.2% GA	sphere	$22.0 \pm 0.1^\gamma$			$118 \pm 0^\delta$
+ 0.2% MG	rod-like		$406 \pm 9^\lambda$	21.4 ± 0.1	$780 \pm 5^\mu$
+ 0.2% EG	rod-like		$674 \pm 25^{\pi,o}$	21.2 ± 0.2	$1,269 \pm 11^\pi$
+ 0.2% PG	rod-like		609 ± 17^v	21.6 ± 0.1	$1,414 \pm 10^\theta$
+ 0.2% BG	rod-like		$718 \pm 23^\pi$	21.8 ± 0.2	$1,438 \pm 14^\theta$
+ 0.2% OG	rod-like		$812 \pm 32^\rho$	27.3 ± 0.2	$2,340 \pm 33^\omega$
+ 0.2% SA	sphere	$20.5 \pm 0.1^\alpha$			$100 \pm 1^\beta$
+ 0.2% FA	sphere	$20.9 \pm 0.1^\beta$			$105 \pm 0^\gamma$
+ 0.2% pC	rod-like		$287 \pm 8^\eta$	19.7 ± 0.2	$471 \pm 6^\lambda$
+ 0.2% CA	rod-like		$482 \pm 15^\mu$	20.6 ± 0.1	829 ± 6^v

CTAB emulsifier shows strongest interaction with antioxidant

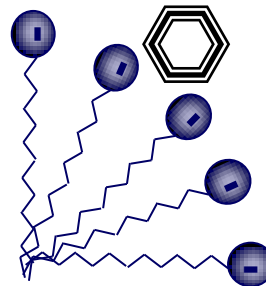
Location by Solubilization



⇒ Solubilization in palisade layer
of CTAB micelles



⇒ Solubilization in head group
area of Brij micelles



⇒ Solubilization in Stern layer
of SDS micelles

Antioxidant: action and location

Anionic surfactant - SDS. Antioxidants locate at Stern layer and act as cosolvent.

Smaller micelles from decreasing of dielectric constant due to the cosolvent.

Weak H-acceptor properties and driving force is hydrophobic effects.

Nonionic surfactant – Brij 58. Antioxidants locate at polyoxyethylene chain and act as alcohol cosolvent.

Lose the surfactant structure, polyoxyethylene chain is more closer to hydrophobic core and hydrophilic micellar shell is thinner. Decreases slightly aggregation number of micelles and number of molecules per surface.

Cationic surfactant – CTAB. Antioxidants locate at palisade layer and act as cosurfactants.

Antioxidants leads to sphere-to-rod transition, increases the aggregation number of micelles and makes tighter packing of CTAB molecules. It means that Coulomb forces are weakened. Confirmed by NMR. CTAB is strong H-bond acceptor.

Heins A., Garamus V. M., Steffen B., Stöckmann H., Schwarz K.

“Impact of Phenolic Antioxidants on Structural Properties of Micellar Solutions”

Food Biophysics, 2006, v. 1, P. 189-201.

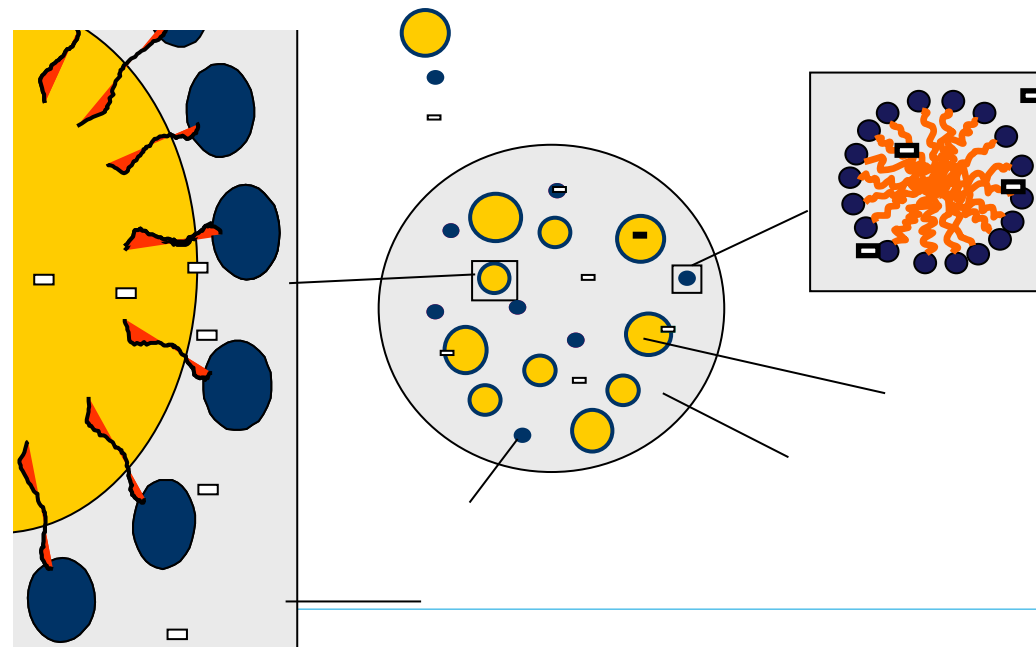
Interface Structure of Emulsifier

Activity of antioxidant is inverse proportional to strength of interaction between antioxidant and emulsifier.

Good antioxidant activity is strongly depended on proximity of antioxidant and radical which is controlled by emulsifier at interface – results of electron spin resonance

Heins et al. (2007) *Lipids*, 42: 561 - 572

Task is to get concentration (structure) of emulsifier at oil droplet interface with aqueous solution



Partitioning of Emulsifiers: Methods

Droplet size: Laser diffraction – Helos Laser Diffraction instrument. Samples were diluted ~ 1500-fold. Dilution did not affect of droplet size. **Hydrodynamic radius and total interfacial area.**

Ultrafiltration: Centrifugal devices with 2 pore sizes. Regenerated cellulose membranes with nominal molecular weight cut-off (MWCO) of 3 kDa (Centricon YM3, Millipore) – **molecular aqueous solution**. MWCO of 100 kDa (Centricon YM100) - **SDS micelles + monomers**. Inorganic membranes with pore size 20 nm (VestaSpin micro, Whatman) – **CTAB micelles + monomers**. Equilibration steps. Room temperature.

Dialysis: Side-by-side diffusion cells. Cellulose ester membrane with MWCO of 3.5 kDa – **molecular aqueous solution** and 300 kDa (SpectraPor, Spectrum Laboratories, USA) - **SDS micelles + monomers**. 72 h at room temperature.

Quantification: SDS - 4 μ L filtrate or permeate were added to 3 mL of 45 μ M methyl orange and 35 cetyl pyridinium bromide. **CTAB** - 30 μ l of filtrate or permeate were added to 3 ml of a 60 μ M methyl orange solution in degassed deionised water/ethanol (80/20), absorbance at 465 nm.

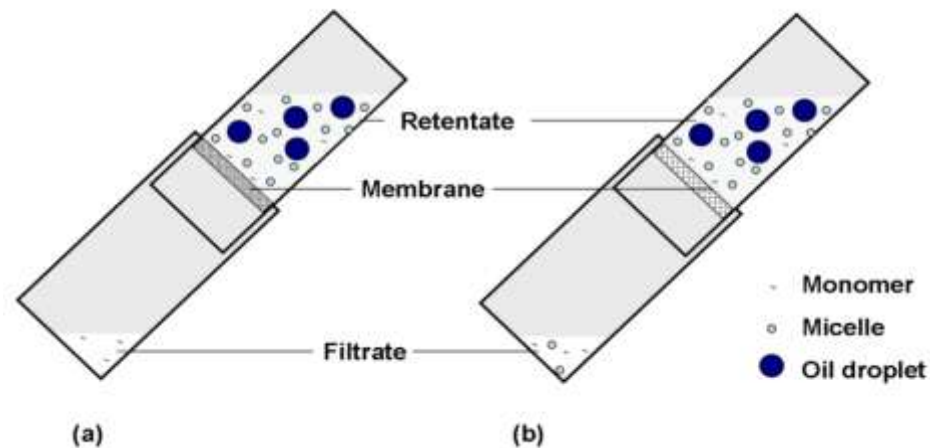
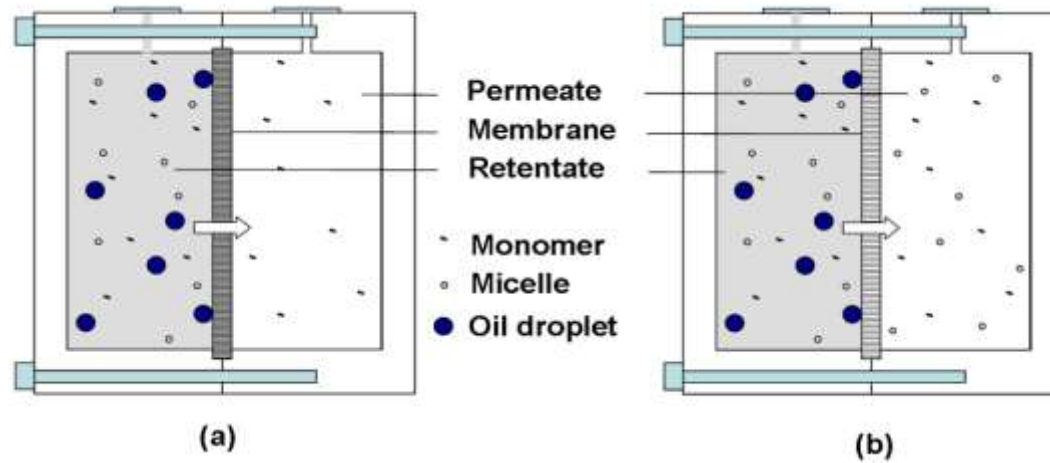
Partitioning of Emulsifiers: Methods

SANS as nondestructive (nonseparation) method. IFT analysis as results $p(r)$ - pair distance distribution function, radius of gyration R_g and scattering at “zero angle” $I(0)$. (i) the trace scattering from large particles was approximated by the power law $q^{-\alpha}$ and (ii) the studied domains were spherical 3D objects. Best fits - when $\alpha = 4$, which correlates to a smooth, sharp interface of large emulsion aggregates.

$$C_{\text{tot}} = C_{\text{int}} + C_{\text{mic}} + C_{\text{mon}}$$

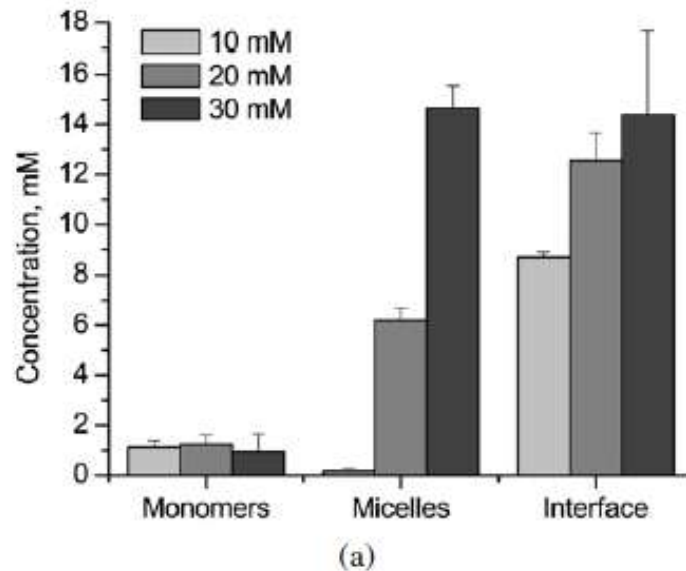
The total emulsifier concentration c_{tot} can be fractionated into the o/w interfacial concentration c_{int} , the micellar concentration c_{mic} and the monomer concentration c_{mon} .

Dialysis vs. Ultrafiltration of Emulsions

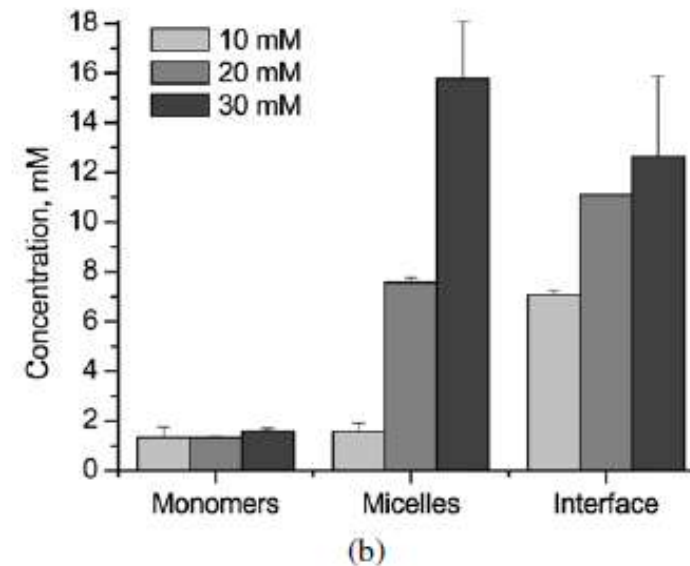


Partitioning of Emulsifiers: SDS

Ultrafiltration



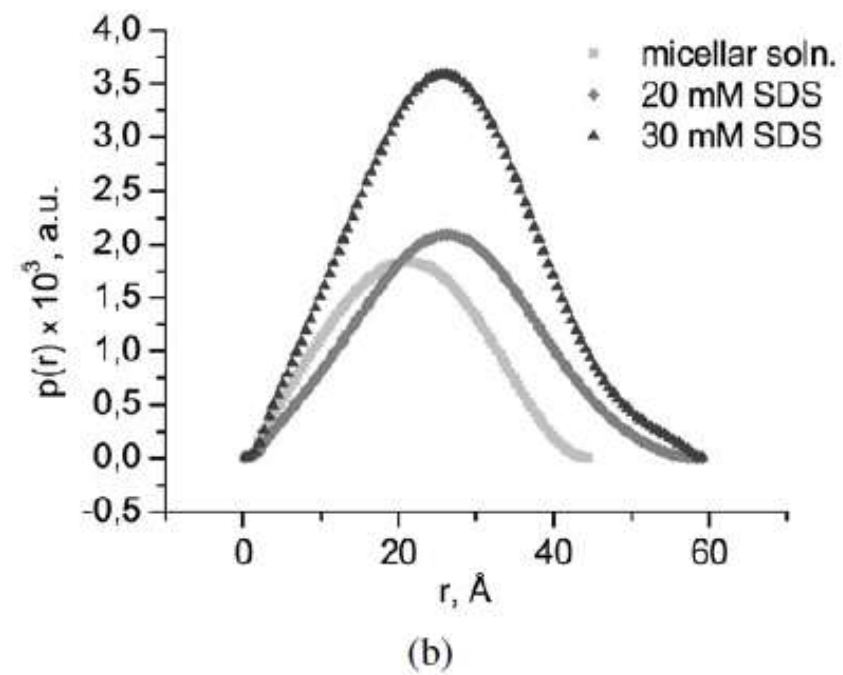
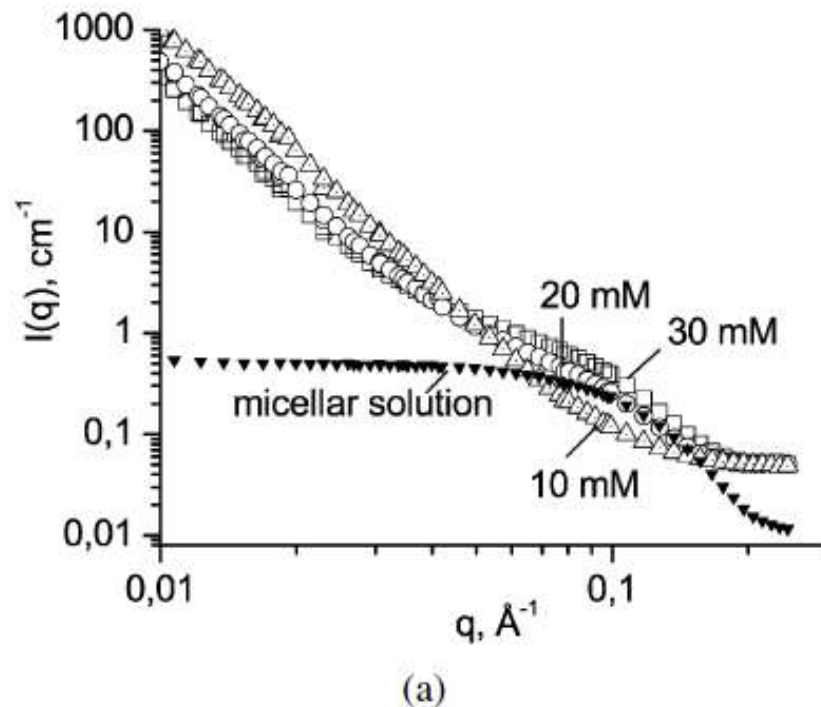
Dialysis



Partitioning of SDS in o/w emulsions determined by (a) ultrafiltration and (b) dialysis

- ✓ The monomer concentrations by UF were in the range of 1 mM (slightly above CMC) and by dialysis in the range of 1–2 mM (1-2xCMC).
- ✓ Micellar concentrations increased from 0.2 to 16.2 mM (UF) and 1.6-15.9 mM (dialysis).
- ✓ Interfacial SDS concentration rose with an increase of total SDS from 10 to 20 mM, but an increase of total SDS from 20 to 30mM did not affect the SDS concentration at the o/w interface.

Partitioning of Emulsifiers: SDS by SANS

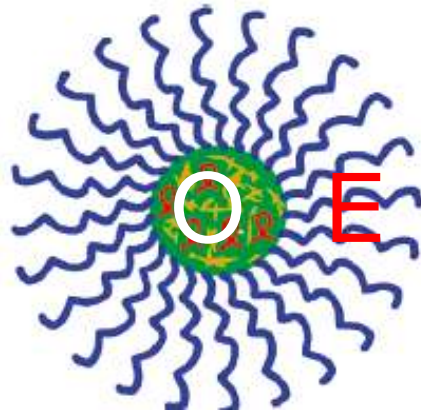


(a) Scattering curves and (b) pair distance distribution functions of emulsions with 10, 20 and 30 mM SDS and of a micellar solution of SDS in D₂O

Increasing SDS concentrations led to the appearance of a shoulder in high q -range - the presence of micelles

Partitioning of Emulsifiers: Methods

Swollen micelle



Emulsifier shell (L) and oil core (R_{core}).

Molecular volumes V_{mol} , scattering length densities per unit mass $\Delta\rho$, chain lengths L and cmc of SDS, CTAB and oil in deuterium buffer solution

	V_{mol} (\AA^3) ^a	$\Delta\rho \times 10^{-10}$ (cm/g) ^b	L (\AA) ^c	cmc (mmol/l) ^d
SDS	413	-5.95	16.7	0.8
CTAB	606	-5.76	21.7	0.096
Oil	1800	-6.63	-	-

R_g and $I(0)$

$$R_{\text{mic}} = \sqrt{\frac{5}{3}} R_g,$$

$$V_{\text{mic}} = \frac{4}{3} \pi R_{\text{mic}}^3.$$

$$R_{\text{core}} = R_{\text{mic}} - L$$

$$V_{\text{core}} = \frac{4}{3} \pi R_{\text{core}}^3$$

$$\phi_{\text{em}} = \frac{V_{\text{mic}} - V_{\text{core}}}{V_{\text{mic}}}$$

$$\phi_{\text{oil}} = 1 - \phi_{\text{em}}.$$

$$\Delta\rho_{\text{mic}} = \phi_{\text{em}} \Delta\rho_{\text{em}} + \phi_{\text{oil}} \Delta\rho_{\text{oil}}$$

$$I(0) = \eta \Delta\rho_{\text{mic}}^2 V_{\text{mic}}$$

$$c_{\text{mic}} = \frac{\phi_{\text{em}} \eta}{V_{\text{mol}} N_a}$$

Partitioning of Emulsifiers: Micelle Structure

Fitted results of the SANS measurements

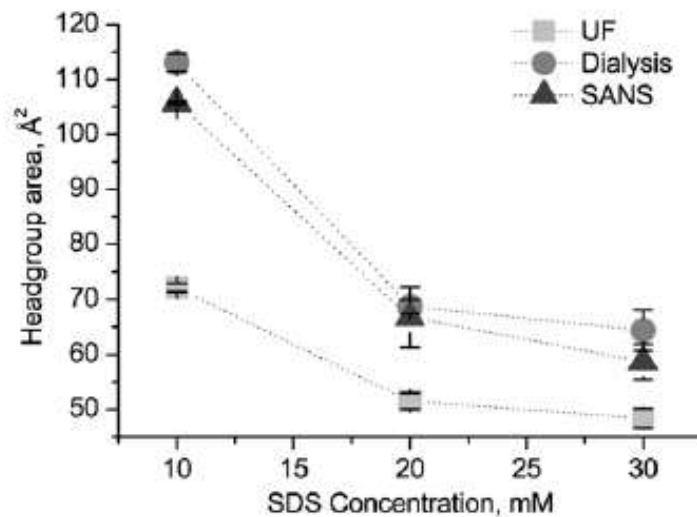
	$I(0)$ (cm ⁻¹) ^a mean ± s.d. ^f	R_g (Å) ^a mean ± s.d. ^f	R_{mic} (Å) ^b mean ± s.d. ^f	$\eta \times 10^3$ ^c mean ± s.d. ^g	c_{mic} (mM) ^d mean ± s.d. ^g	c_{int} (mM) ^e mean ± s.d. ^g
SDS solution	0.57 ± 0.01	16.2 ± 0.1	20.9 ± 0.1			
Emulsions						
10 mM SDS	n.d.	n.d.	n.d.	0	0	9.2 ± 0.07
20 mM SDS	0.74 ± 0.04	20.3 ± 0.4	26.2 ± 0.5	2.75 ± 0.18	10.52 ± 0.69	8.68 ± 0.69
30 mM SDS	1.30 ± 0.04	20.3 ± 0.4	26.2 ± 0.5	4.83 ± 0.15	18.47 ± 0.59	10.73 ± 0.59
CTAB solution	1.69 ± 0.01	20.1 ± 0.1	25.9 ± 0.1			
Emulsions						
10 mM CTAB	n.d.	n.d.	n.d.	0	0	9.9 ± 0.01
20 mM CTAB	2.20 ± 0.1	27.9 ± 0.5	36.0 ± 0.6	3.32 ± 0.15	7.34 ± 0.04	12.56 ± 0.04
30 mM CTAB	3.3 ± 0.1	27.6 ± 0.4	35.6 ± 0.5	5.15 ± 0.16	11.85 ± 0.04	18.05 ± 0.04

In the emulsion with 10 mM of emulsifier - no micelles were detected.

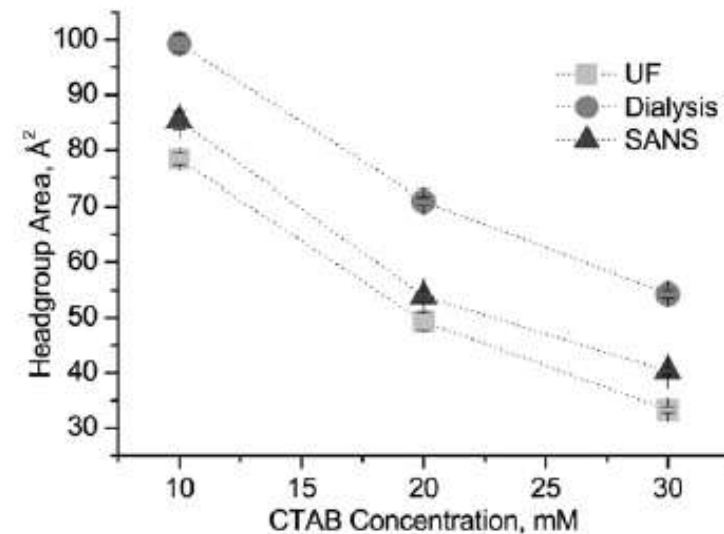
Radius of micelle in microemulsion is larger than in binary emulsifier/buffer system – **incorporation of oil**

Area per Molecule at Oil Droplet Interface

SDS



CTAB



SANS has been successfully used for validation of dialysis and UF

Ultra filtration method is considered to be more accurate method - due to better control

Oehlke K., Garamus V. M., Heins A., Stöckmann H., Schwarz K.

“The partitioning of emulsifiers in o/w emulsions: A comparative study of SANS, ultrafiltration and dialysis”

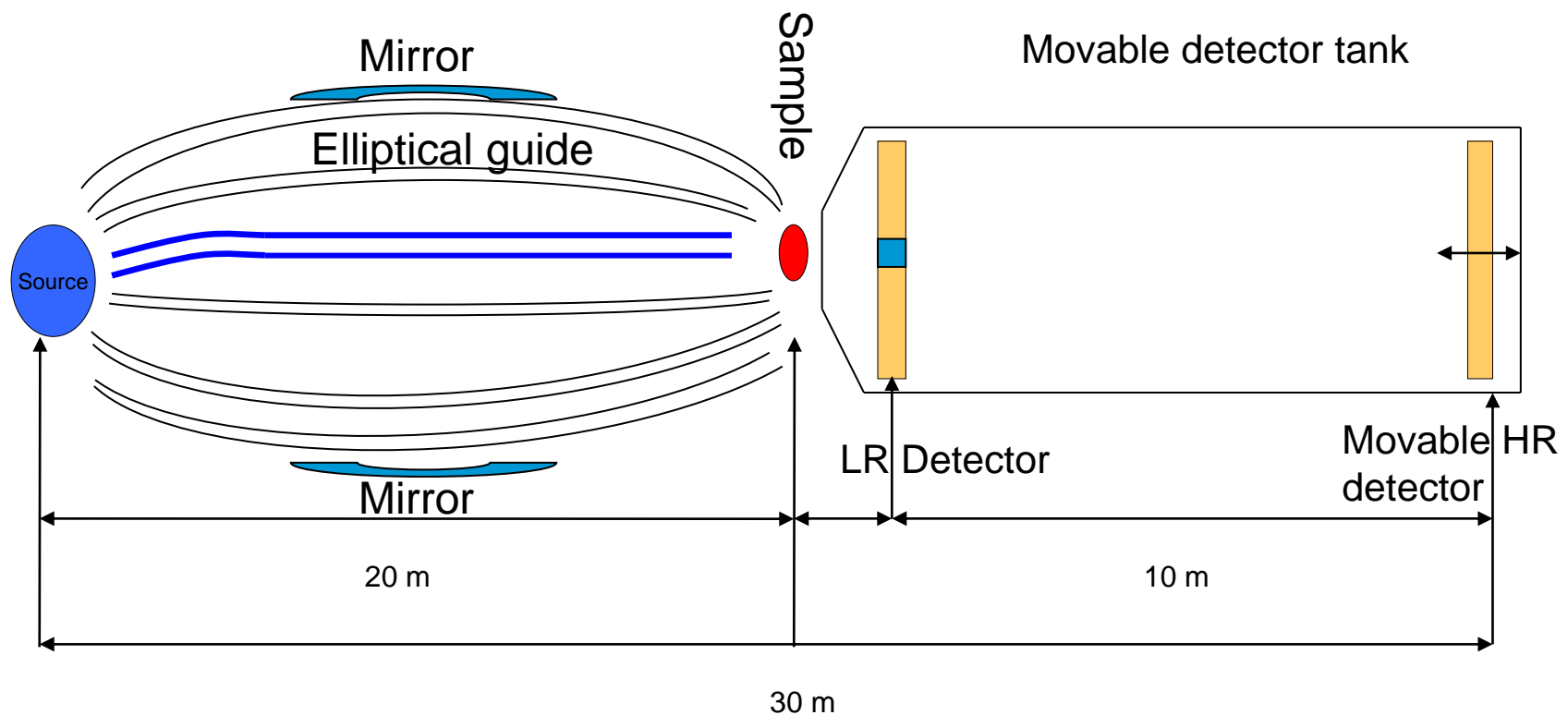
Journal of Colloid and Interface Science, 2008, v. 322, P. 294–303

Small Sample SANS at ESS

Beam sizes of $2 \times 2 \text{ mm}^2$ or below (reduction to $50 \times 50 \text{ }\mu\text{m}^2$)

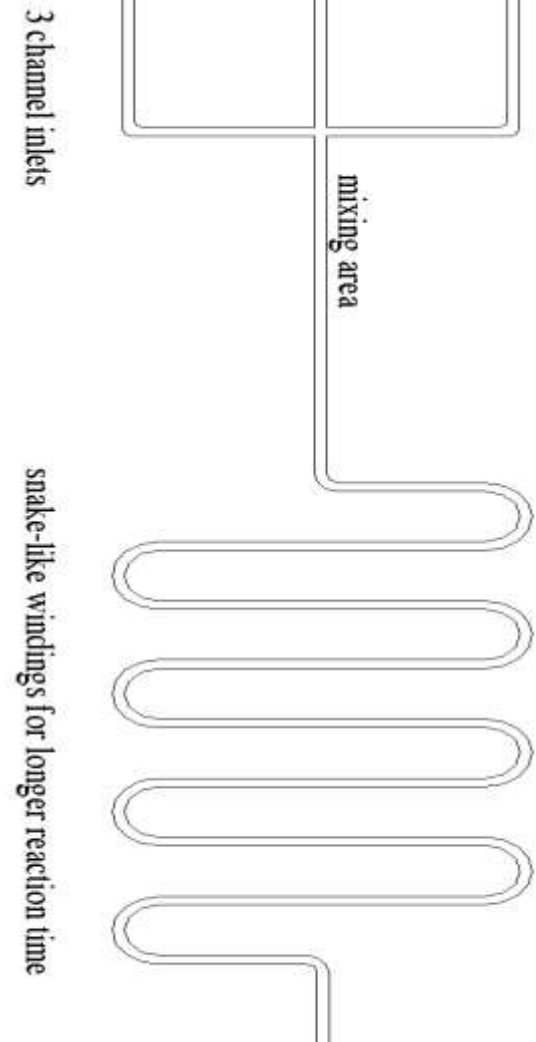
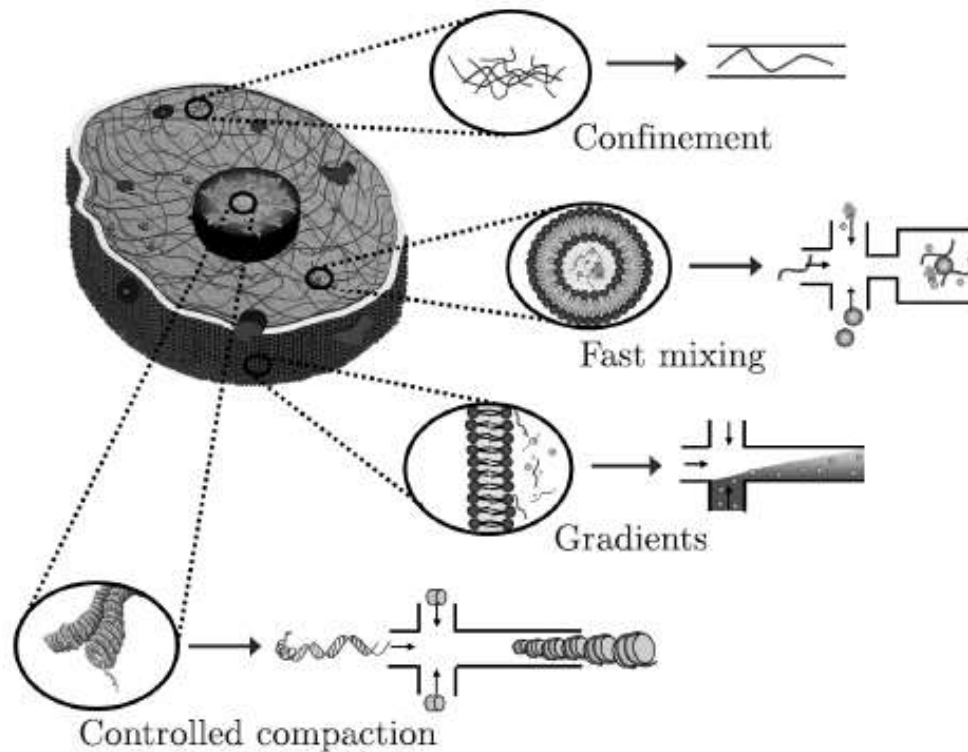
Q-range from $10^{-3} - 1 \text{ \AA}^{-1}$

Speed of measurements as normal size sample ($10 \times 10 \text{ mm}^2$) at ILL



Sample position

Micro fluid chip



Evans et al., Bull. Pol. Ac.: Tech., 2007, 55, 217

Diameter of channel ~ 100 μm